

# Supramolecular Assembly of Hypervalent Iodine Macrocycles and Alkali Metals

Krishna Pandey,<sup>1</sup> Lucas X. Orton,<sup>1</sup> Grayson Venus<sup>1</sup>, Waseem A. Hussain,<sup>1</sup> Toby Woods<sup>2</sup>, Lichang Wang,<sup>1</sup> and Kyle N. Plunkett<sup>1\*</sup>

<sup>1</sup>School of Chemical and Biomolecular Sciences, Southern Illinois University, Carbondale. Carbondale, IL 62901

<sup>2</sup>George L. Clark X-ray Facility and 3M Materials Laboratory, University of Illinois at Urbana-Champaign, Urbana, IL, 61801, United States

kplunkett@chem.siu.edu

## Abstract

This study explores the solution- and solid-state assembly of phenylalanine based hypervalent iodine macrocycles (HIMs) with lithium and sodium cations. The metal cation binding of HIMs was evaluated by addition of lithium tetrakis(pentafluorophenyl)borate ethyl etherate (Li)BARF and sodium tetrakis[3,5-bis(trifluoromethyl)phenyl] borate (Na)BARF. The relatively electron rich, outwardly projected carbonyl oxygens of the HIM co-crystallize with the cations into bent supramolecular architectures. Both crystal structures show a pattern of assembly between HIM and metal cation in 2:1 ratio. While association with sodium leads to a polymer-like network, the lithium crystal structure was limited to dimeric assemblies of HIM. In the lithium coordinating complex, the oxygen-lithium-oxygen bond angle is approximately 98.83°, displaying a closer arrangement of two HIMs. In contrast, the sodium complex exhibits a more open orientation of two HIMs with an oxygen-sodium-oxygen bond angle close to 167.98°. Lastly, a comparative study of association constants and binding energies for phenylalanine based HIM with (Li)BARF and (Na)BARF are presented.

**Introduction** Supramolecular chemistry is emerging as a pivotal area of research in both medicinal and material chemistry that opens the avenue for new functionalized materials for their use in medical devices or therapeutics,<sup>1</sup> drug delivery,<sup>2</sup> supramolecular sensing,<sup>3</sup> purification,<sup>4</sup> and separation.<sup>5, 6</sup> The interactions in supramolecular assemblies are driven by well know hydrogen-bonding, hydrophobic interactions, electrostatic interactions and pi-pi stacking.<sup>7, 8</sup> The supramolecular chemistries of hypervalent iodine systems that involve secondary bonding to form a higher order molecular assemblies are yet to be fully explored. The term ‘hypervalency’ is defined as the ability of an atom to expand its valence shell beyond the limits of a Lewis octet.<sup>9</sup> Among several hypervalent-capable atoms (e.g., Cl, I, S, P, etc.), hypervalent iodine reagents have gained the most interest in organic chemistry owing to their unique reactivities, low toxicity, high stability, ease of handling, and economical alternative to heavy metal reagents.<sup>10, 11</sup> Hypervalent iodine compounds exist as trivalent ( $\lambda^3$ -iodanes) or pentavalent ( $\lambda^5$ -iodanes) species. The  $\lambda^3$ -iodanes have an T-shaped structure,<sup>12</sup> with the energetically preferred arrangement of the two most electronegative heteroatoms at axial positions resulting in a three-center four electron bond.<sup>13, 14</sup> In this unique ‘T’ configuration, the bond length between iodine and one of the heteroatoms is influenced by the bond distance of the other heteroatom and is responsible for the stabilization of the hypervalent iodine system.<sup>12</sup> In addition to these covalent bonding interactions, additional secondary bonding (e.g., red dotted bonds between iodine and oxygen in phenylalanine based

hypervalent iodine macrocycle in benzene system in Figure 1A) can arise in these systems from neighboring atom lone pairs.

Secondary bonding is characterized as those interactions that involve intermolecular hypervalent connections with lengths shorter than the sum of the van der Waals radii between a heavy p-block element and an electron pair donor (typically O, N, S, or halogen).<sup>15</sup> Secondary I---O interactions have been found to help assemble higher order supramolecular hypervalent iodine macrocycles.<sup>16-18</sup> Examples of hypervalent iodine macrocycles (HIMs) include those synthesized by Ochiai,<sup>16</sup> Tykwinski and Zhdankin,<sup>17</sup> and our group's extension of those works. (Figure 1A-B).<sup>18, 19</sup> The main driving force for the assembly of HIM is attributed to the weak, yet additive, secondary bonding interactions between electron deficient iodine atom and electron rich oxygen atoms. These examples highlight new possibilities in material science owing to their unique assembly via secondary bonding as well as their dynamic assembly and disassembly.

In our previous report,<sup>18</sup> we synthesized new phenylalanine based HIMs and demonstrated the dynamic nature of the HIM assemblies in solution by assembly and disassembly by addition and the removal of anions (e.g., chloride, bromide, fluoride, and cyanide), respectively (Figure 1A). Furthermore, we showed that the HIMs are dynamic in nature even in the absence of additional anions with the monomers exchanging between macrocycles to participate in dynamic covalent chemistry based on secondary bonding in these systems. As a demonstration of even higher supramolecular assemblies, we also showed pi-extended HIMs enable the co-assembly of Buckminster fullerene into long range assembled structures (Figure 1B).<sup>19</sup>

In this contribution, we explored the cation binding abilities of HIMs with first group alkali metals such as lithium and sodium. Through a series of crystallographic experiments, we demonstrate that HIMs coordinate with alkali metals through the periphery carbonyl oxygens via metal-oxygen bonding to form a higher order metal coordinated hypervalent iodine based macrocyclic complex. Furthermore, we have experimentally and computationally compared the association constants of lithium tetrakis(pentafluorophenyl)borate ethyl etherate (Li)BARF and sodium tetrakis[3,5-bis(trifluoromethyl)phenyl] borate (Na)BARF in the phenylalanine HIM system.

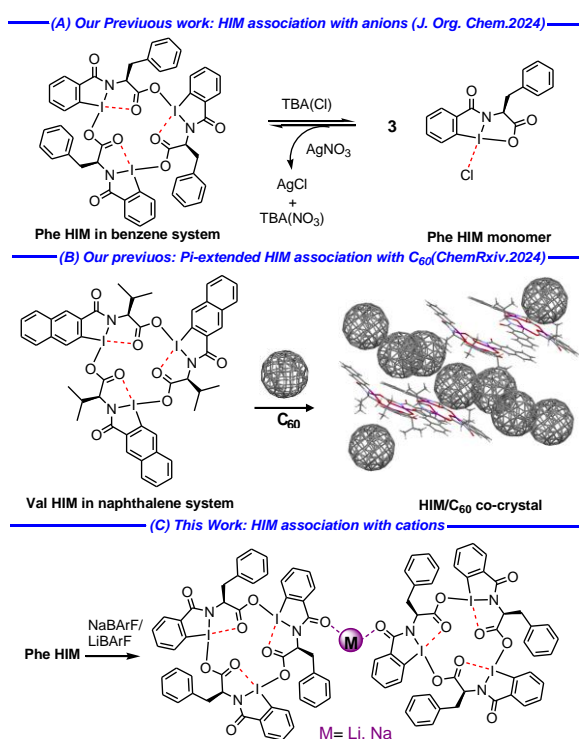
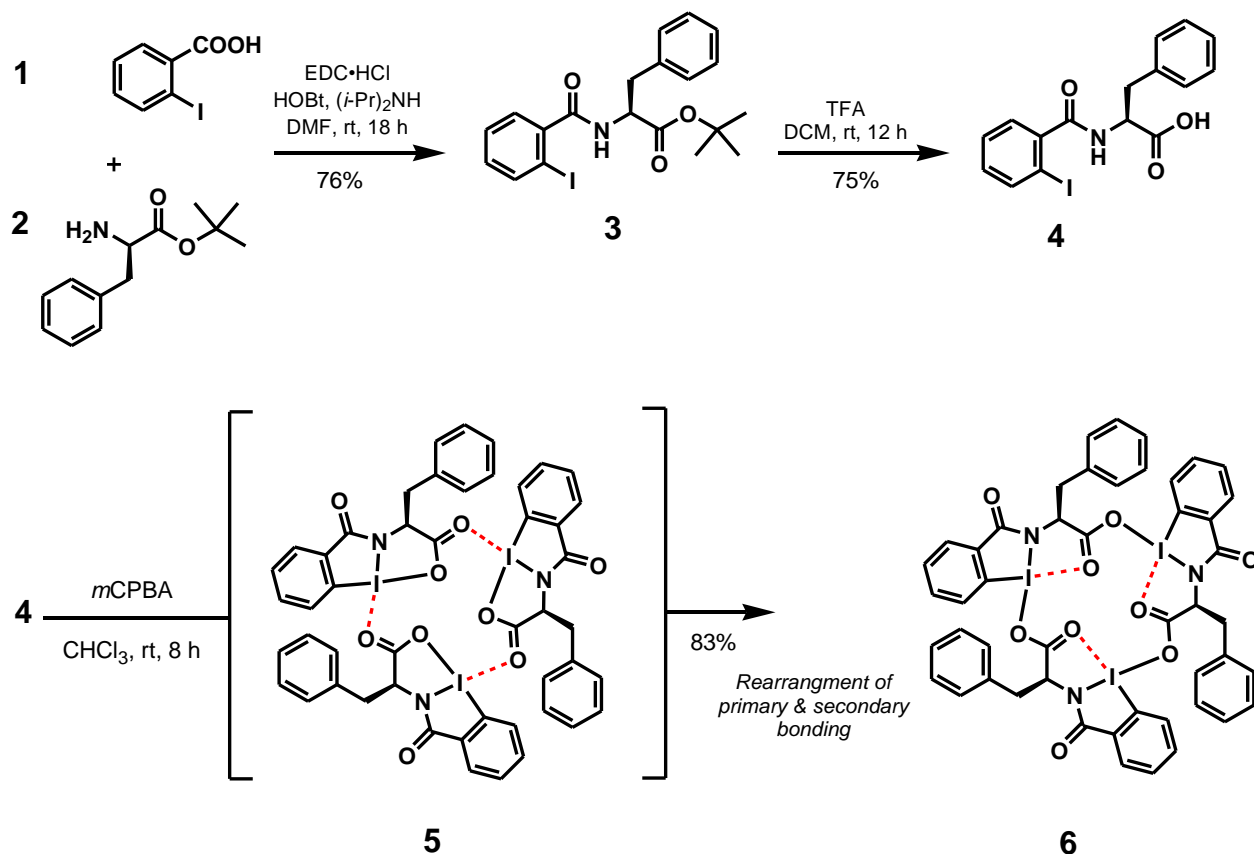


**Figure 1.** (A) Our previous work: Assembly and disassembly of phenylalanine hypervalent iodine macrocycles (**Phe HIM**) through anion coordination. (B) Another work on pi-extended hypervalent iodine macrocycle and their supramolecular assembly with Buckminster fullerene (C) This work: Association of Phe HIM with group first alkali metal cations. Secondary bonds are highlighted in red.

## Results and Discussion

We have reported the synthesis of several variations of valine and phenylalanine based HIMs that are based on benzene- naphthalene- and anthraquinone systems.<sup>18,19</sup> This study employed phenylalanine and iodo-benzoic acid based HIM system for this study owing to its simplicity in synthesis and ease of crystal growth. Following our previously established synthetic route, phenylalanine based HIM were synthesized in three steps (Scheme 1) by utilizing commercially available 2-iodobenzoic acid and L-Phe-OtBu as starting materials. An amide coupling reaction between 2-iodobenzoic acid and L-Phe-OtBu.HCl (**2**) gave **3**, which was deprotected with trifluoroacetic acid to give HIM precursor **4**. The synthesis of phenylalanine HIM was accomplished by oxidation of intermediate **4** with 3-chloroperoxybenzoic acid. The final HIM **6** was fully characterized by <sup>1</sup>H and <sup>13</sup>C spectroscopy and high-resolution mass spectrometry (HRMS).

**Scheme 1.** Synthesis of phenylalanine based hypervalent iodine macrocycle <sup>a</sup>.



<sup>a</sup> Rearrangement of secondary bonding gives the more stable “T” binding motif around hypervalent iodine leads to a stabilized macrocycle.

Previously,<sup>18</sup> phenylalanine HIM **6** was isolated in crystalline form in two different molecular conformations. In conformer I (**6-I**, Figure 2, bottom), all three benzyl groups oriented towards the interior of the macrocycle. In contrast, conformer II (**6-II**, Figure 2, top) features two benzyl groups projecting inward and one benzyl group projecting outward denoted by an asterisk. Furthermore, the resulting crystal structure reveals that HIM **6** is also a distorted planar macrocyclic system consisting of the amino acids carbonyl oxygen facing inside the ring. All three benzyl groups are located above a single plane (more figures are provided in supporting information, Figure S11). In addition, the crystal structure also demonstrates that the three iodine atoms, three carbonyl carbon atoms and six oxygen atoms circumscribe a small bowl-like cavity within the macrocycle. With the consideration of all primary and secondary bonds, the small cavity is highlighted by blue color in the chemical structure of phenylalanine HIM as shown in Figure 3(left) (More figures SI). Despite the core's composition of six electron-rich oxygen atoms, we hypothesized that the bowl-like macrocyclic cavity is electron-deficient in nature owing to the presence of three electron-deficient iodine atoms within the macrocycle's framework. To better understand the electrophilic environment of the macrocyclic cavity, we have calculated the Mulliken charges on each atom of Phe HIM **6**. To analyze the resultant charge of the macrocycle's cavity, we considered the charge distribution on three iodine atoms, three

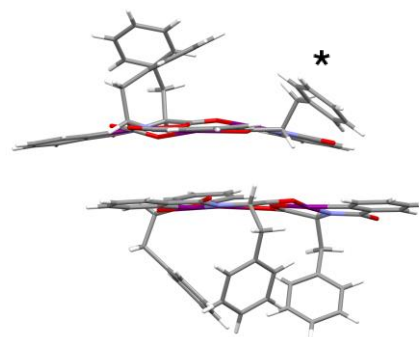


**Figure 2.** Two conformations of the HIM were found. One conformation projected all three benzyl groups in a vertical arrangement **6-II** (bottom) while the second conformation (**6-I**) projected only two vertically. one benzyl ring is pointed outside as highlighted by \*(top). Oxygen, nitrogen and iodine atoms are denoted by red, light blue and purple color respectively.

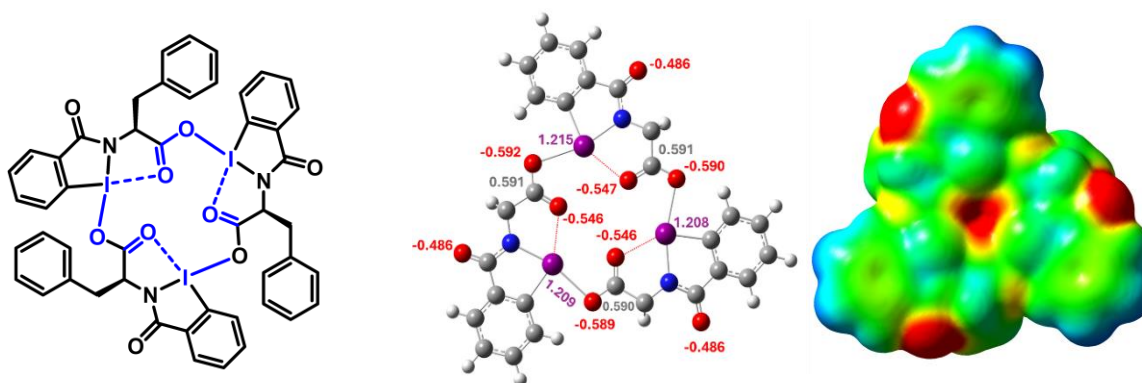


**Figure 3.** Left) Chemical structure of HIM **6**: Three iodine atoms and three inward projected ester carbonyls circumscribe the small cyclic core represented by blue color. Three carbonyl amides project outward. Middle) DFT image of **6** displaying the distribution of Mulliken charges on iodine (purple), oxygen (red) and carbon (grey); benzyl groups are omitted for clarity. Right) Calculated electrostatic potential map showing the electrophilic core highlighted by less intense red color surrounded by green color of **6**. Periphery oxygens (formerly the carbonyl of benzoic acid) are electron rich highlighted by more intense red color.

carbonyl carbon atoms and six oxygen atoms that constitute a small cavity within the macrocycle. The Mulliken charge distribution diagram of HIM **6** (Figure 3, middle) shows that the summation of the overall charge on three oxygen atoms facing towards the center of the macrocycle is somewhat lower than the summation of charge of the three iodine atoms. The resultant charge calculated from three iodine, three carbonyl carbons and six oxygen atoms constituting HIM cavity

is  $1.994 e^-$ , suggesting that the central core of macrocycle is electrophilic in nature. In addition, DFT results show the three outwardly projected carbonyl oxygens (formerly the carbonyl of benzoic acid) are negatively charged and can potentially bind or interact with metal cations. Figure 3 (right) shows the calculated electrostatic potential map with the area of the electrophilic cavity of HIM in lighter red (less intense) color that suggests lower electron density. In contrast, the three outwardly projected carbonyl oxygens (formerly the carbonyl of benzoic acid) are dark red (more intense) in color demonstrating the higher overall electron density of that region. Additional information of the electrostatic potential map with color code is provided in the supporting information (Figure SI14).

We recently reported that anions of tetrabutylammonium salts such as  $F^-$ ,  $Cl^-$ ,  $Br^-$  and  $CN^-$  disrupt the secondary bonding in the HIMs and initiate the disassembly of the HIM trimer into a HIM monomer. The HIMs were found not to interact with tetrabutylammonium nitrate, signifying a lack of association between the HIM and the bulky cation (tetrabutylammonium) or the non-nucleophilic anion (nitrate). With these observations, and the previous report of possible cation binding via mass spectrometry experiments,<sup>17</sup> we were intrigued by the potential of HIM binding smaller cations such as lithium and sodium. While the previous authors suggested metal cations bind at the oxygen rich core in a similar fashion to crown ethers, our hypothesis diverged and considered alternative binding sights including the exterior of the HIMs. Recently, Huber and coworkers<sup>20</sup> showed hypervalent iodine (III) compounds were not impacted by non-coordinating BARF cations. Upon this inspiration, we employed (Li)BARF and (Na)BARF as salt sources to investigate the association of HIMs with metal cations.

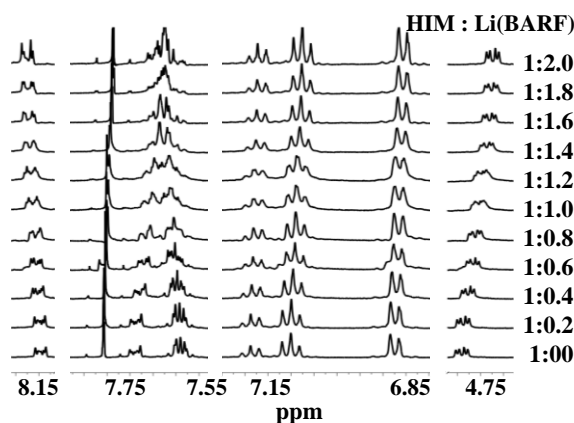


**Figure 4.**  $^1H$  NMR titration experiment of **6** with (Li)BARF at an incremental equivalency in  $CDCl_3$  and  $(CD_3)_2CO$ .

NMR titration of HIM **6** with (Li)BARF led to distinct shifting of signals with the successive addition of salt. Figure 4 shows a titration of **6** with increasing equivalents of (Li)BARF. The most dramatic changes included the proton multiplet at 7.750 ppm shifting upfield and the multiplet at 7.60 ppm shifting downfield and merging into a single multiplet when approximately 1:1 ratio of HIM to salt was added. Additional titration data are provided in supporting information (Figure SI4 and SI5). Similar, yet less dramatic shifts were observed for the other aromatic and aliphatic protons. Alternatively, titration with (Na)BARF showed much smaller, yet measurable, movement in the aromatic proton signals upon equivalent salt additions (Supporting Information, Figure SI6, SI7). These results suggest that there are new associative processes occurring in the presence of both (Li)BARF and (Na)BARF. The larger magnitude of changes with the addition of (Li)BARF in comparison to (Na)BARF suggests a stronger association and is presumably owing to the difference in size and bonding strength of the cations.

To further understand the complexation with metal cations, separate co-crystals of HIM **6** with (Li)BARF and (Na)BARF were obtained by vapor diffusion of diethyl ether into acetone. Single

crystals suitable for XRD quality were obtained in both cases (Figure 5). Unlike the previous assumption of metal coordination at the macrocycle core,<sup>17</sup> the crystal structures reveal complexation of both cations at the periphery of the macrocycle. Both **6**/(Li)BARF and **6**/(Na)BARF crystallized in an orthorhombic system with a P212121 space group, where the unit

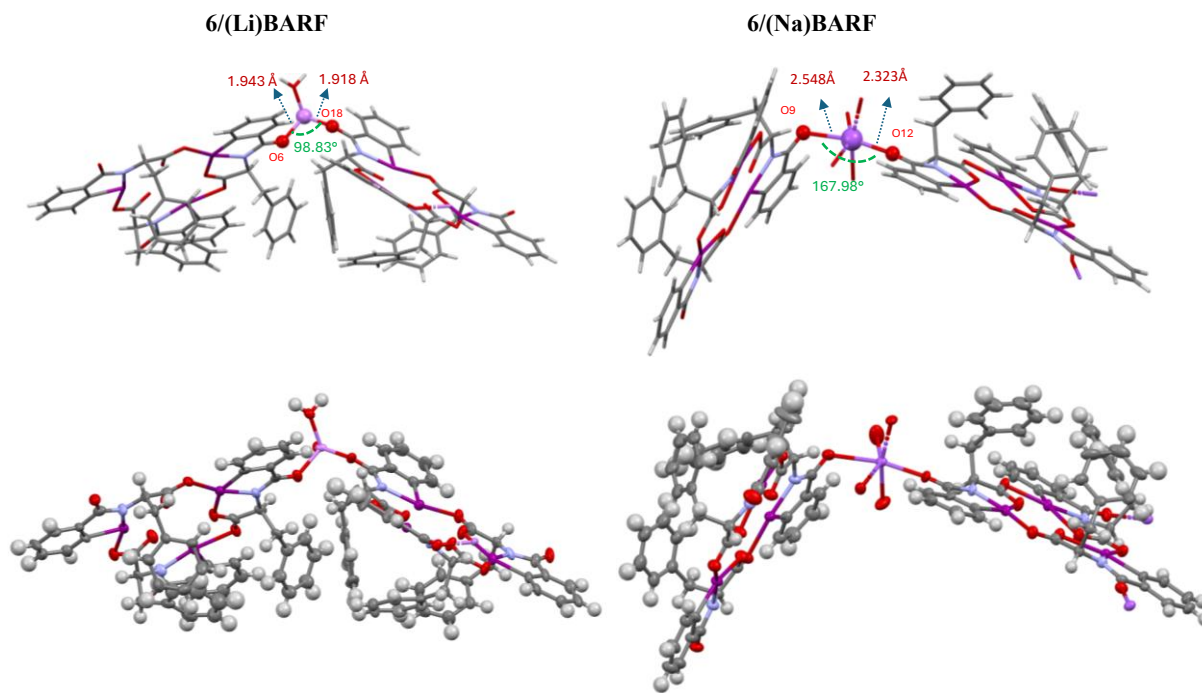


**Figure 5.** Crystal structures of HIM **6** and (Li)BARF (Left) and (Na)BARF (Right). BARF anion is omitted for clarity. Nitrogen, oxygen, Iodine, and metal (lithium or sodium) atoms are denoted by light blue, red, purple, and lavender color respectively. Thermal ellipsoids drawn at 50% probability.

cell of each complex contains two molecules of HIM for every metal BARF. Details of the crystal structure data set can be found in ESI. The overall macrocycle structures are analogous to the single crystal structure of the previously reported phenylalanine HIMs alone (Figure 2). For the **6**/(Li)BARF crystal, the phenylalanine HIMs exist in two different molecular conformations analogous to **6-I** and **6-II** (Figure 6) with differences arising in the location of the projected benzyl groups. For **6**/(Na)BARF complex, the repeating unit shows that both phenylalanine HIMs exhibit in same conformation (e.g., **6-I**) where all three benzyl groups oriented toward the interior of the macrocycle (Figure SI).

From the single crystal data set, we observed that a lithium ion is coordinated with two variations of the phenylalanine macrocycles (**6-I** and **6-II**) through the outwardly projected carbonyl oxygens (O6 from **6-I** and O18 from **6-II**) via oxygen-metal bonds (Figure 5). The bond distance between O6 - Li is 1.943 Å, which is slightly longer than the bond distance between O18 - Li of 1.918 Å. The overall

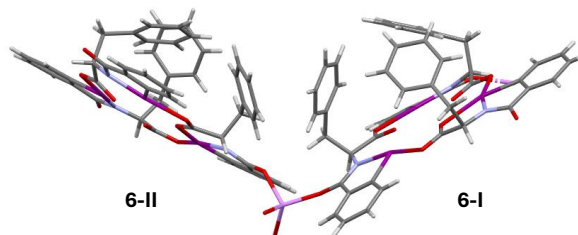


**Figure 6.** Alternative view of crystal structure of HIM and (Li)BARF complex. BARF anion is omitted for clarity. Nitrogen, oxygen, Iodine, and lithium atoms are denoted by light blue, red, purple, and lavender color respectively. Conformer **6-II** displays two benzyl groups are projected in and a benzyl group projected out. Conformer **6-I** displays all benzyl groups projected interior of the macrocycle.

structure is a bent dimer with the two phenylalanine HIM structures arranged in close geometry with a O6-Li-O18 bond angle of 98.83°. In contrast, the Na<sup>+</sup> incorporated co-crystal structure is different than the Li<sup>+</sup> co-crystal, even though the unit cell is almost the same. In this complex, the Na<sup>+</sup> is similarly coordinated with two phenylalanine macrocycles through amide moiety carbonyl oxygen (O9 from one **6-I** and O12 from second **6-I**). However, the bond distances between oxygen and the metal are significantly longer for Na<sup>+</sup> versus Li<sup>+</sup>. The O9 - Na distance is 2.548 Å while the O12 - Na is 2.323 Å. On average, the average difference in bond lengths between Li<sup>+</sup> and Na<sup>+</sup> is ~0.5 Å. Unlike the Li<sup>+</sup> complex, the Na<sup>+</sup> complex grows into a polymer-like network. While the overall structure forms a polymer, the molecular repeating unit consists of two HIM **6** for every (Na)BARF. Though only the smallest unit of the chain is shown in Figure 5, the ratio of the HIM **6** to (Na)BARF remains 2:1 upon applying the same number of symmetry operators to the chain. The Na<sup>+</sup> bond angles are more linear than Li<sup>+</sup> with O9-Na-O12 bond angle of 167.98°.

To better understand the association process in this HIM system, the proton <sup>1</sup>H NMR titration data was used to determine the association constants for metal coordination. Two stock solutions were prepared with one containing a concentration of 2.83 mM of the macrocycle (HIM) in a mixture of deuterated chloroform and acetone. The second stock solution contained the metal BARF at a concentration of 10 times that of the HIM concentration. Gradually adding the metal BARF stock solution to HIM stock solution in NMR tubes allowed the host-to-guest ratio to be varied while keeping the host concentration constant. With crystallographic confirmation of a 2:1 H.G complex, titration data was fitted using a 2:1 model of HIM to Metal BARF (Figure 7).<sup>21,22</sup> The calculated cooperative association constants for **6** with (Li)BARF are 0.09 M<sup>-1</sup> and 21522 M<sup>-1</sup>. The cooperative association constants for HIM with (Na)BARF were found to be considerably lower with associations of 68 M<sup>-1</sup> and 115 M<sup>-1</sup>. Notably, the association constant magnitude correlated with the strength of the respective metal oxygen bond.

The relatively high Ka value seen for Li<sup>+</sup> as compared to Na<sup>+</sup> cation is presumed to result from difference in atom size. The Li<sup>+</sup>, being smaller in size binds more strongly with HIM than the Na<sup>+</sup> resulting in the higher binding constants. To gain further insight into the difference in binding constants as well as the isolation of two distinct molecular conformation of phenylalanine HIM **6** (Figure 1), DFT calculations were performed. The details of DFT calculations are shown in Table 1. For DFT

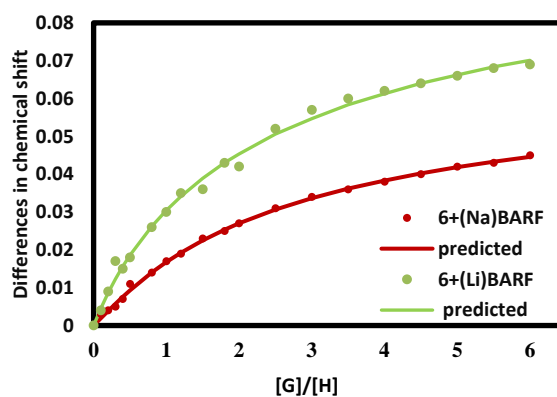


**Figure 7.** Isotherms of **6** titrated with (Na)BARF or (Li)BARF. The solid lines are the predicted model fits for each curve. [H] is defined as concentration of HIM.

System	Binding Energy (kJ/mol)	Binding Constant (M <sup>-1</sup> )
HIM <b>6-I</b>	-297.05	
HIM <b>6-II</b>	-237.31	
Li Complex <b>7 (6-I,6-II)</b>	-1029.87	0.09, 21522
Li Complex <b>8 (6-I,6-I)</b>	-1029.69	
Na Complex <b>9 (6-I, 6-II)</b>	-896.39	
Na Complex <b>10 (6-I,6-I)</b>	-897.77	68, 115

**Table 1.** Binding energies and binding constants for HIM **6** with (Li)BARF and (Na)BARF.

calculations, we assigned two HIM macrocycles per (Li)BARF as found in the co-crystal. Li<sup>+</sup> complex **7** represents the complex consisting of HIM in two different molecular conformations (**6-I** and **6-II**), whereas Li<sup>+</sup> complex **8** represents a complex consisting of both macrocycles in the same molecular conformation (e.g., **6-I** and **6-I**). Similarly, Na<sup>+</sup> complex **9** represents the complex consisting of HIM in two different molecular conformations (**6-I** and **6-II**), whereas Na<sup>+</sup> complex **10** represents a complex consisting of both HIM in same molecular conformation (**6-I** and **6-I**). Without any metal coordination, DFT suggests conformer **6-I** is more stable than conformer **6-II** by ~60 kJ/mol. However, upon complexation with Li<sup>+</sup>, both complexes (**7** and **8**) are remarkably similar in energy with the difference of less than 1 KJ/mol. This very small energy difference should be too small for marked differences in the arrangement of groups in space. The overlaid image of lithium complex **7** and **8** (Figure 8) shows the similar arrangement of all groups on plane except for one benzyl ring (highlighted by \*) in complex **7** that faces outside the interior of the macrocycle. A similar trend was seen in the HIM - Na<sup>+</sup> crystals where complex **9** and complex **10** are similar in energy with a difference of less than 1.5 KJ/mol. While both Li<sup>+</sup> and Na<sup>+</sup> crystals were prepared in similar conditions, the difference in the resulting crystal structure (e.g., location of benzyl rings) could arise from a difference in the overall nucleation events of a given crystal and not necessarily a difference in energy between conformations. DFT result of the binding energy of the two metals shows that the isolated Li<sup>+</sup> complex **7** (1029.87 KJ/mol) is more stable than the Na<sup>+</sup> complex (897.77 KJ/mol). This significant energy difference supports the observed stronger binding of Li<sup>+</sup> in these systems. The higher binding constant of for Li<sup>+</sup> cation is consistent with the correlation between binding constants and binding energies for 2:1 model.<sup>23</sup>

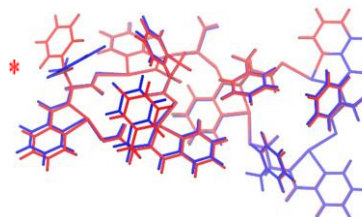


**Figure 8.** Lithium complex (**7**) overlaid with lithium complex (**8**). Lithium (**7**) and lithium (**8**) are highlighted in red and blue color respectively. In lithium complex **7**, one benzyl ring is pointed outside as highlighted by red color\*.

## Conclusions

In conclusion, we have explored the binding of hypervalent iodine macrocycles with two first alkali metals. Analysis of association constants reveals that, upon addition of (Li)BARF and (Na)BARF, the Li<sup>+</sup> binds stronger than Na<sup>+</sup> cation with the macrocycle. Alternative to a previous report, the metal cations bind to the periphery of the macrocycle and not to the electrophilic (yet oxygen rich) core of the macrocycle.

## ASSOCIATED CONTENT

### Data Availability Statement

The data underlying this study are available in the published article and its Supporting Information.

**Supporting Information.** Detailed experimental procedures, NMR spectra, X-ray crystallography details. “This material is available free of charge via the Internet at.....”

## AUTHOR INFORMATION

Corresponding Author

\* *Kyle N. Plunkett* – *School of Chemical and Biomolecular Sciences, Southern Illinois University, Carbondale, Illinois, 6290, United states* Email: [kplunkett@chem.siu.edu](mailto:kplunkett@chem.siu.edu) or <https://orcid.org/0000-0002-5691-7876>

### Authors

**Krishna Pandey** – *School of Chemical and Biomolecular Sciences, Southern Illinois University, Carbondale, Carbondale, Illinois 62901, United States*

**Lucas X. Orton** – *School of Chemical and Biomolecular Sciences, Southern Illinois University, Carbondale, Carbondale, Illinois 62901, United States*

**Grayson Venus** – *School of Chemical and Biomolecular Sciences, Southern Illinois University, Carbondale, Carbondale, Illinois 62901, United States*

**Waseem A. Hussain** – *School of Chemical and Biomolecular Sciences, Southern Illinois University, Carbondale, Carbondale, Illinois 62901, United States*

**Toby J. Woods** – *George L. Clark X-ray Facility and 3M Materials Laboratory, University of Illinois at Urbana-Champaign, Urbana, Illinois 61801, United States; orcid.org/0000-0002-1737-811X*

**Lichang Wang** – *School of Chemical and Biomolecular Sciences, Southern Illinois University, Carbondale, Carbondale, Illinois 62901, United States*

### Author Contributions

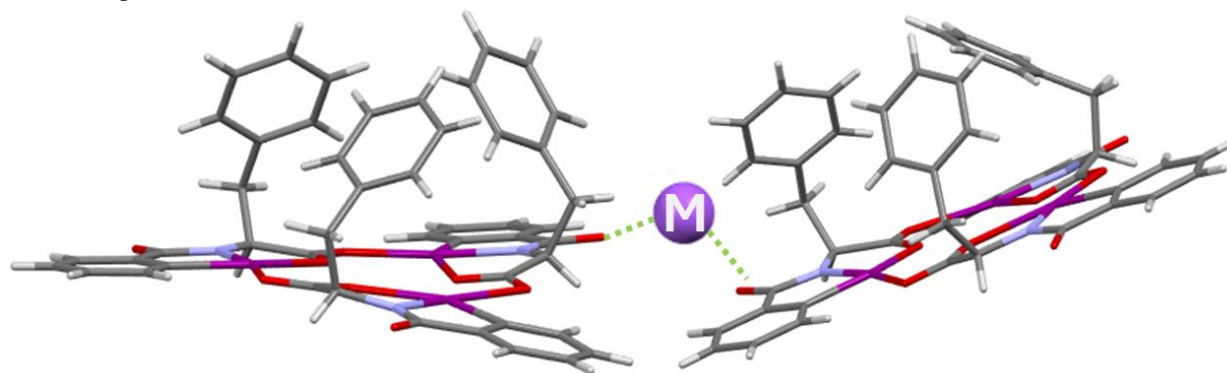
KP, LXO, WAH and KNP contributed to synthetic aspects of the work. KP prepared crystals for X-ray analysis, performed titration experiments, performed isotherm analysis, and devised the reversibility experiment. GV and LW performed DFT calculations. TJW obtained and solved the X-ray structures. KNP envisioned the experimental direction of the project. KP and KNP wrote the manuscript and edited by all authors. All authors have given approval to the final version of the manuscript.

### ACKNOWLEDGMENT

We thank the National Science Foundation (#2003654), the American Chemical Society Petroleum Research Fund (61467-ND1) and Dr. Bob Gower and Mrs. Beth Gower (Gower Fellowship 2023) for support of this work.

### Notes

The authors declare no competing financial interest.



## References

1. Webber, M. J.; Langer, R., Drug delivery by supramolecular design. *Chemical Society Reviews* **2017**, *46* (21), 6600-6620.
2. Uekama, K.; Hirayama, F.; Irie, T., Cyclodextrin Drug Carrier Systems. *Chemical Reviews* **1998**, *98* (5), 2045-2076.
3. de Silva, A. P.; Vance, T. P.; West, M. E.; Wright, G. D., Bright molecules with sense, logic, numeracy and utility. *Org Biomol Chem* **2008**, *6* (14), 2468-80.
4. Zhang, G.; Lin, W.; Huang, F.; Sessler, J.; Khashab, N. M., Industrial Separation Challenges: How Does Supramolecular Chemistry Help? *Journal of the American Chemical Society* **2023**, *145* (35), 19143-19163.
5. Wilson, A. M.; Bailey, P. J.; Tasker, P. A.; Turkington, J. R.; Grant, R. A.; Love, J. B., Solvent extraction: the coordination chemistry behind extractive metallurgy. *Chemical Society Reviews* **2014**, *43* (1), 123-134.
6. Brenner, W.; Ronson, T. K.; Nitschke, J. R., Separation and Selective Formation of Fullerene Adducts within an M118L6 Cage. *Journal of the American Chemical Society* **2017**, *139* (1), 75-78.
7. Amabilino, D. B.; Smith, D. K.; Steed, J. W., Supramolecular materials. *Chemical Society Reviews* **2017**, *46* (9), 2404-2420.
8. Atwood, J. L.; Lehn, J. M., *Comprehensive supramolecular chemistry*. 1st ed.; Pergamon: New York, 1996.
9. Musher, J. I., The Chemistry of Hypervalent Molecules. *Angewandte Chemie International Edition in English* **1969**, *8* (1), 54-68.
10. Stang, P. J.; Zhdankin, V. V., Organic Polyvalent Iodine Compounds. *Chem Rev* **1996**, *96* (3), 1123-1178.
11. Yoshimura, A.; Zhdankin, V. V., Advances in Synthetic Applications of Hypervalent Iodine Compounds. *Chemical Reviews* **2016**, *116* (5), 3328-3435.
12. Ochiai, M.; Sueda, T.; Miyamoto, K.; Kiprof, P.; Zhdankin, V. V., trans Influences on hypervalent bonding of aryl lambda(3)-iodanes: their stabilities and isodesmic reactions of benziodoxolones and benziodazolones. *Angew Chem Int Ed Engl* **2006**, *45* (48), 8203-6.
13. Pimentel, G. C., The Bonding of Trihalide and Bifluoride Ions by the Molecular Orbital Method. *The Journal of Chemical Physics* **1951**, *19* (4), 446-448.
14. Weinhold, F.; Landis, C. R., *Valency and Bonding: A Natural Bond Orbital Donor-Acceptor Perspective*. Cambridge University Press: 2005.

15. Alcock, N. W., Secondary Bonding to Nonmetallic Elements. In *Advances in Inorganic Chemistry and Radiochemistry*, Emeléus, H. J.; Sharpe, A. G., Eds. Academic Press: 1972; Vol. 15, pp 1-58.
16. Ochiai, M.; Masaki, Y.; Shiro, M., Synthesis and structure of 1-alkynyl-1,2-benziodoxol-3(1H)-ones. *The Journal of Organic Chemistry* **1991**, *56* (19), 5511-5513.
17. Zhdankin, V. V.; Kuposov, A. E.; Smart, J. T.; Tykwinski, R. R.; McDonald, R.; Morales-Izquierdo, A., Secondary Bonding-Directed Self-Assembly of Amino Acid Derived Benziodazoles: Synthesis and Structure of Novel Hypervalent Iodine Macrocycles. *Journal of the American Chemical Society* **2001**, *123* (17), 4095-4096.
18. Pandey, K.; Arafin, S.; Jones, E.; Du, Y.; Kulkarni, G. C.; Uddin, A.; Woods, T. J.; Plunkett, K. N., Assembly and Disassembly of Supramolecular Hypervalent Iodine Macrocycles via Anion Coordination. *The Journal of Organic Chemistry* **2024**, *89* (11), 7437-7445.
19. Pandey, K.; Arafin, S.; Venus, G.; Jones, E.; Du, Y.; Dumre Pandey, M.; Awais, T.; Wang, L.; Plunkett, K. N., Pi-Extended Hypervalent Iodine Macrocycles and their Supramolecular Assembly with Buckminster Fullerene, ChemRxiv, **2024**, 10.26434/chemrxiv-2024-13rlh.
20. Heinen, F.; Engelage, E.; Cramer, C. J.; Huber, S. M., Hypervalent Iodine(III) Compounds as Biaxial Halogen Bond Donors. *Journal of the American Chemical Society* **2020**, *142* (19), 8633-8640.
21. <http://supramolecular.org/> (accessed 2000).
22. Brynn Hibbert, D.; Thordarson, P., The death of the Job plot, transparency, open science and online tools, uncertainty estimation methods and other developments in supramolecular chemistry data analysis. *Chemical Communications* **2016**, *52* (87), 12792-12805.
23. Tiwari, L.; Leach, C.; Williams, A.; Lighter, B.; Heiden, Z.; Roll, M. F.; Moberly, J. G.; Cornell, K. A.; Waynant, K. V., Binding Mechanisms and Therapeutic Activity of Heterocyclic Substituted Arylazothioformamide Ligands and Their Cu(I) Coordination Complexes. *ACS Omega* **2024**, *9* (35), 37141-37154.